Biochimica et Biophysica Acta, 736 (1983) 11–27
Elsevier

BBA 71878

CHARACTERIZATION OF SODIUM AND PROTON FLOWS IN SUB-BACTERIAL PARTICLES OF *HALOBACTERIUM HALOBIUM* IN TERMS OF NONEQUILIBRIUM THERMODYNAMICS

SHULAMIT COOPER, ISAAC MICHAELI and S. ROY CAPLAN

Departments of Membrane Research and of Polymer Research, Weizmann Institute of Science, Rehovot (Israel)

(Received February 8th, 1983)
(Revised manuscript received July 1st, 1983)

Key words: Nonequilibrium thermodynamics; Na^+-H^+ exchange; Potential jump; Stoichiometry; (Halobacterium halobium)

A thermodynamic characterization of the Na^+-H^+ exchange system in *Halobacterium halobium* was carried out by evaluating the relevant phenomenological parameters derived from potential-jump measurements. The experiments were performed with sub-bacterial particles devoid of the purple membrane, in 1 M NaCl, 2 M KCl, and at pH 6.5–7.0. Jumps in either pH or pNa were brought about in the external medium, at zero electric potential difference across the membrane, and the resulting relaxation kinetics of protons and sodium flows were measured. It was found that the relaxation kinetics of the proton flow caused by a pH-jump follow a single exponential decay, and that the relaxation kinetics of both the proton and the sodium flows caused by a pNa-jump also follow single exponential decay patterns. In addition, it was found that the decay constants for the proton flow caused by a pH-jump and a pNa-jump have the same numerical value. The physical meaning of the decay constants has been elucidated in terms of the phenomenological coefficients (mobilities) and the buffering capacities of the system. The phenomenological coefficients for the Na^+-H^+ flows were determined as differential quantities. The value obtained for the total proton permeability through the particle membrane via all available channels, $L_H = (\partial J_{H+}/\partial \Delta pH)_{\Delta\psi,\Delta pNa}$, was in the range of 850–1150 nmol $H^+ \cdot (mg\ protein)^{-1} \cdot h^{-1} \cdot (pH\ unit)^{-1}$ for four different preparations; for the total Na^+ permeability, $L_{Na} = (\partial J_{Na^+}/\partial \Delta pNa)_{\Delta\psi,\Delta pH}$, it was 1620–2500 nmol $Na^+ \cdot (mg\ protein)^{-1} \cdot h^{-1} \cdot (pNa\ unit)^{-1}$; and for the proton 'cross-permeability', $L_{HNa} = (\partial J_{H^+}/\partial \Delta pNa)_{\Delta\psi,\Delta pH}$, it was 220–580 nmol $H^+ \cdot (mg\ protein)^{-1} \cdot h^{-1} \cdot (pNa\ unit)^{-1}$, for different preparations. From the above phenomenological parameters, the following quantities have been calculated: the degree of coupling (q), the maximal efficiency of Na^+-H^+ exchange (η_{max}), the flow and force efficacies (ϵ) of the above exchange, and the admissible range for the values of the molecular stoichiometry parameter (r). We found $q \leqslant 0.4$; $\eta_{max} \leqslant 5\%$; $0.36 \leqslant r \leqslant 2$; $\epsilon_{J_{Na^+}} \leqslant 1.3 \cdot 10^5$ $\mu mol \cdot (RT\ unit)^{-1}$ at $J_{Na} = 1$ $\mu mol\ Na^+ \cdot (mg\ protein)^{-1} \cdot h^{-1}$; and $\epsilon_{\Delta pNa} \leqslant 5 \cdot 10^4$ $\Delta pNa \cdot (mg\ protein) \cdot h \cdot (RT\ unit)^{-1}$ at $\Delta pNa = 1$ unit, for different preparations.

Introduction

The osmoregulatory properties of *Halobacterium halobium* have aroused special interest because of the unique natural environment of this bacterium. The *H. halobium* species exists in solutions containing 4 M NaCl as well as a few mM KCl [1–4]. Under such extreme osmotic conditions only few species survive. Several reviews discussing the unique properties of these bacteria have been published [5–8]. In this work we studied the characteristics of proton and Na^+ transport in sub-bacterial particles of *H. halobium* in the dark.

Abbreviations: Mes, 2-(*N*-morpholino)ethanesulfonic acid; Pipes, piperazine-*N*,*N*′-bis(2-ethane sulfonic acid); Hepes, *N*-2-hydroxyethylpiperazine-*N*′-2-ethanesulfonic acid; $TPMP^+$ Br^-, triphenylmethylphosphonium bromide; TPB^-, tetraphenylboron; DCCD, *N*,*N*′-dicyclohexylcarbodiimide; FCCP, carbonyl cyanide *p*-trifluoromethoxyphenylhydrazone.

Some extensive studies on the Na^+-H^+ exchange system in the same sub-bacterial preparation have already been carried out previously in our laboratory [9–12] and by the group of Lanyi et al. [8,13–17]. It was found that under illumination, sodium ions are extruded against their own electrochemical potential gradient, from the interior into the external medium. This extrusion is made possible by the coupling of the Na^+-flow with the flow of protons, when the latter are driven down their electrochemical potential gradient. The proton electrochemical potential gradient ($\tilde{\mu}^{ext}_{H^+} > \tilde{\mu}^{int}_{H^+}$) in the sub-bacterial particles is created by a light-driven reaction catalyzed by the bacteriorhodopsin pigment [11,18–20] (and also Refs. 5–8) and, in the case of the intact bacteria, also by respiration [21–25]. Use of the energy stored in the electrochemical potential of protons, for active extrusion of sodium ions from the interior of the cells, has been observed in all other bacterial systems studied so far, such as: *Streptococcus faecalis*, *Escherichia coli*, *Staphylococcus aureus* and *Micrococcus denitrificans* [26–28]. An attempt has been made to evaluate the H^+-Na^+ exchange stoichiometry in the *H. halobium*. The general conclusion based on different techniques [9,11,14,15,17] was that the stoichiometric ratio ($r = H^+/Na^+$) is larger than 1, and it was assumed that $r = 2$. In view of the recent discovery of halorhodopsin, suggested to be a light-driven primary Na^+-pump [29–32], the analysis of measurements obtained under illumination should be reevaluated. However, the inhibitory effect of $\Delta\psi$ repressors ($TPMP^+$ and TPB^-) on Na^+-transport under illumination can still be explained only in terms of an electrogenic exchange ($r > 1$) [9,14]. In any case, halorhodopsin may pump Cl^- rather than Na^+ [33].

It may be in order to mention that the build-up of a Na^+-gradient in the *H. halobium* is also related to Na^+-amino-acid symport [8,14,16,17,34–37] and to Na^+-Ca^+ antiport [38].

Following the above qualitative observations on the patterns of Na^+ and proton flows, this paper presents further work leading to a quantitative characterization of the Na^+-H^+ exchange system, based on the approach of irreversible thermodynamics. This approach has already been applied to several other systems. To quote a few examples, it has been applied to the mitochondrial system, in order to characterize quantitatively the oxidative phosphorylation process [39–41], to the frog-skin system, in order to characterize the chemically driven Na^+-transport [42–47], to the Ehrlich-cell system in order to characterize Na^+/2-aminoisobutyrate cotransport [48,49], and to the bacteriorhodopsin system, to characterize the light-driven proton pump [39,50]. In the present paper experimental results are reported on the flows of sodium ions and of protons in sub-bacterial particles of *H. halobium* devoid of bacteriorhodopsin, as affected by the chemical potential differences of these ions. The resulting phenomenological coefficients are then used for the calculation of the degree of coupling (q), of the maximal efficiency (η_{max}) of energy-conversion in the pumping process of Na^+-extrusion, of the flow ($\epsilon_{J_{Na^+}}$) and force ($\epsilon_{\Delta pNa}$) efficacies, and of the theoretically admissible values for a possible mechanistic stoichiometry of the H^+/Na^+ exchange (r) [18,40,51,52].

The experimental approach in this work is based on the 'potential-jump' method, and involves measurement of the flow-relaxation kinetics. The acid pulse pH relaxation has been extensively discussed in the literature (see, for example, Refs. 53–56). As shown below, this method provides a novel way for the determination of the buffering capacities of the vesicles *.

List of symbols

J_i: The net-flow of the ion indicated by the subscript ($i = H^+, Na^+$). J_i is positive for flows from the external medium into the vesicles.

$\Delta\tilde{\mu}_i$: The electrochemical potential difference of the respective ion, across the vesicle membrane. We take $\Delta\tilde{\mu}_i > 0$ when $\tilde{\mu}^{ext}_i > \tilde{\mu}^{in}_i$ ($i = H^+, Na^+$).

pH: $pH = -\log \gamma_{H^+} \cdot [H^+]$

pNa: $pNa = -\log \gamma_{Na^+} \cdot [Na^+]$
where γ is the activity coefficient.
Since all the experiments were performed at constant ionic strength, $\Delta \log \gamma$ could be neglected, so that ΔpNa

* In the literature (see, for example, Refs. 53,55,56) it is emphasized that measurements of external pH changes make it possible to calculate changes in internal pH provided the internal buffering capacity is known. Here we show that changes in external pH observed in a relaxation experiment can be used to calculate the internal buffering capacity itself. In this calculation knowledge of the internal pH is not required.

(or, $pNa^{ext\ II} - pNa^{ext\ I}$) was computed from the concentrations.

ΔpNa, ΔpH: ΔpNA and ΔpH indicate in all cases the difference between the external and the internal pNa or pH, respectively. When a pH-jump or a pNa-jump (in the external medium) was introduced, it is always designated as ($pH^{ext\ II} - pH^{ext\ I}$), or ($pNa^{ext\ II} - pNa^{ext\ I}$), respectively.

L'_{ij}: The phenomenological conductance coefficients, correlating J_i and $\Delta\tilde{\mu}_j$, $L'_{ij} \equiv (\partial J_i/\partial\Delta\tilde{\mu}_j)_{\Delta\tilde{\mu}}$, according to Eqns. 1 and 2.

L_{ij}: The phenomenological conductance coefficients correlating J_i with ΔpH or with ΔpNa, at $\Delta\psi = 0$; we have, $L_{ij} = 2.3\ RTL'_{ij}$.

K_i: The flow-relaxation constants for J_i ($i = H^+, Na^+$).

q: the degree of coupling between the Na^+ and H^+ flows.

η_{max}: the maximal efficiency of energy conversion between the Na^+ and H^+ flows.

ϵ_{J_i} and $\epsilon_{\Delta\tilde{\mu}_i}$: The flow and force efficacies, respectively,

$$\epsilon_{J_i} \equiv \left| \left(\frac{J_i}{J_j \Delta\tilde{\mu}_j} \right)_{\Delta\tilde{\mu}_i = 0} \right|$$

$$\epsilon_{\Delta\tilde{\mu}_i} \equiv \left| \left(\frac{\Delta\tilde{\mu}_i}{J_j \Delta\tilde{\mu}_j} \right)_{J_i = 0} \right|$$

r: the 'mechanistic stoichiometry' in the H^+-Na^+ exchange system.

n_i^{int}: the amount of the respective vesicular ion, per unit of vesicular protein ($i = H^+, Na^+$).

n_i^{ext}: the amount of the respective ion in the external medium, per unit of vesicular protein ($i = H^+, Na^+$).

$n_i^{int\infty}$, $n_i^{ext\infty}$: as above, but at equilibrium.

int: in the vesicles.

ext: in the external medium.

t: time.

Theoretical considerations

The flows of protons (J_{H^+}) and of sodium ions (J_{Na^+}) through the membrane of sub-bacterial particles of *H. halobium* can be represented by the following expressions, for a linear region, when there is no coupling with the flows of K^+, Cl^-, and water, which are also present in the system [40,51,52]. We have:

$$J_{H^+} = L'_H \Delta\tilde{\mu}_{H^+} - L'_{HNa} \Delta\tilde{\mu}_{Na^+} \quad (1)$$

$$J_{Na^+} = -L'_{NaH} \Delta\tilde{\mu}_{H^+} + L'_{Na} \Delta\tilde{\mu}_{Na^+} \quad (2)$$

where $\Delta\tilde{\mu}$ represents the electrochemical potential difference (external minus internal) of the ion indicated by the subscript. J_{H^+} and J_{Na^+} are taken as positive for flows into the vesicles. When the difference in the electric potential is suppressed ($\Delta\psi = 0$), we have:

$$J_{H^+} = -L_H \Delta pH + L_{HNa} \Delta pNa \quad (3)$$

$$J_{Na^+} = +L_{NaH} \Delta pH - L_{Na} \Delta pNa \quad (4)$$

where ΔpH and ΔpNa indicate differences between external and internal values of the negative logarithms of the respective ionic acitivities. For a linear region far from equilibrium, constant third terms may in principle appear in Eqns. 1–4. However, these terms cancel in Eqn. 5 below and in all our expressions involving L-values, since the latter are defined as differential coefficients.

The phenomenological coefficients (the L-values) uniquely characterize the system under the prevailing experimental conditions *. This description is evidently macroscopic, and is independent of the molecular mechanisms involved.

L_H measurement

The direct overall thermodynamic permeability coefficient for the proton flow across the vesicle membrane (L_H), is defined in Eqn. 3:

$$L_H = -J_{H^+}/\Delta pH \quad \text{at } \Delta\psi = 0 \text{ and } \Delta pNa = 0 \quad (5)$$

An obvious difficulty in the determination of the phenomenological coefficients, according to Eqns. 3 and 4, arises from the need to measure the chemical potentials of Na^+ and of protons in the very small volume of the vesicles. Moreover, an additional difficulty arises because of the fact that the values of the chemical potentials inside the vesicles can be strongly affected by very small flows of protons or sodium ions, because of the very low buffering capacities maintained by the

* Under iso-osmotic conditions and constant Cl^- concentration throughout the system we have only two degrees of freedom for the driving forces, and Eqns. 1–4 are still valid even if there is coupling with K^+ and/or Cl^- flows. In the case of such coupling the L-values in Eqns. 3 and 4 may be regarded as 'apparent' coefficients. The relationship between the apparent and the intrinsic coefficients is readily determined by the Gibbs-Duhem equation.

small vesicular volume. In this work, the need to measure the internal pH and pNa could be totally avoided by applying the 'potential jump' method.

According to this method when applied to L_H measurements, an abrupt change (jump) is produced (at time $t = 0$) in the pH of the external solution, and the proton flows are recorded before and after the occurrence of the potential-jump. The relevant expression for the involved changes in J_{H^+} follow from Eqn. 3, written for conditions just before (I) and just after (II) the potential jump. We have, at $\Delta\psi = 0$,

$$J_H^{I} = -L_H(pH^{ext\,I} - pH^{int\,I}) + L_{HNa}(pNa^{ext\,I} - pNa^{int\,I}) \tag{3a}$$

$$J_H^{II} = -L_H(pH^{ext\,II} - pH^{int\,II}) + L_{HNa}(pNa^{ext\,II} - pNa^{int\,II}) \tag{3b}$$

Evidently at $t = 0$, the chemical potentials of protons and sodium ions in the internal volume have not been affected by the changes introduced in the external solution, so that $pH^{int\,I} = pH^{int\,II}$; similarly, $pNa^{int\,I} = pNa^{int\,II}$. Subtracting Eqn. 3a from Eqn. 3b, we obtain (at $t = 0$)

$$\Delta J_{H^+} = J_{H^+}^{II} - J_{H^+}^{I} = -L_H(pH^{ext\,II} - pH^{ext\,I}) + L_{HNa}(pNa^{ext\,II} - pNa^{ext\,I}) \tag{5a}$$

When the potential jump involves a change in external pH only (so that $pNa^{ext\,II} = pNa^{ext\,I}$), the relationships of Eqn. 5a are reduced to

$$\Delta J_{H^+} = L_H(pH^{ext\,II} - pH^{ext\,I}) \tag{6}$$

The last equation permits the evaluation of L_H from measurements of the change in proton flux (ΔJ_{H^+}) brought about by changes in the external pH ($pH^{ext\,II} - pH^{ext\,I}$) only. It should be emphasized that the ΔpH-jump experiments do not require initial equilibrium conditions at which $J_{H^+} = 0$ and/or $J_{Na} = 0$ and the corresponding potential differences are zero.

In order to calculate ΔJ_{H^+} at $t = 0$, J_{H^+} is measured as a function of time, both before and after the potential jump. This makes it possible to extrapolate the J_{H^+} values to $t = 0$, and thus obtain more reliable values for ΔJ_{H^+}. Analysis of the time dependence of J_{H^+} also provides information on the nature of the flow-relaxation involved. For example, it can determine, whether the relaxation process can be described as a single exponential decay, or whether more complex kinetics are involved. When the flow-relaxation follows a single exponential decay, at ΔpNa = constant, the physical meaning of the decay constant (K_H) follows directly from considerations of time derivatives of Eqn. 3b. According to reference [9], we have the following two alternative expressions for K_H:

$$-K_H \equiv \frac{d\ln(n_{H^+}^{ext} - n_{H^+}^{ext\infty})}{dt} = L_H\left(\frac{pH^{ext} - pH^{ext\infty}}{n_{H^+}^{ext} - n_{H^+}^{ext\infty}} + \frac{pH^{int} - pH^{int\infty}}{n_{H^+}^{int} - n_{H^+}^{int\infty}}\right) \tag{7}$$

or

$$-K_H \equiv \frac{d\ln|J_{H^+}|}{dt} = L_H\left(\frac{dpH^{ext}}{dn_{H^+}^{ext}} + \frac{dpH^{int}}{dn_{H^+}^{int}}\right) \tag{8}$$

From Eqn. 7 we see that the parameter characterizing the flow relaxation is a product of L_H and the sum of the reciprocal values of the mean buffering capacities of the internal and external solutions. A linear logarithmic plot will thus be obtained in the region of a constant product of L_H and the sum of the buffering-capacity terms. This is a weaker restriction than that of constancy of each of the separate terms involved. Analysis of the data in terms of Eqn. 8 has the advantage that it makes no recourse to $n_{H^+}^{ext\infty}$. The latter constant is hard to determine experimentally, and any variation in the assumed value for $n_{H^+}^{\infty}$ affects strongly the shape of the plot of $\ln(n_{H^+} - n_{H^+}^{\infty})$ versus time.

L_{HNa} measurement

The phenomenological coefficient L_{HNa} in Eqn. 3 characterizes the coupling between the proton flow and ΔpNa in the system at $\Delta\psi = 0$. It describes the change in the proton flow because of a change in the Na^+ chemical-potential difference, when the chemical-potential difference of protons is zero. It follows from Eqn. 3 that

$$L_{HNa} = \left(\frac{J_{H^+}}{\Delta pNA}\right)_{\Delta\psi = 0,\,\Delta pH = 0} \tag{9}$$

As in the case of L_H discussed above, the value of L_{HNa} has been obtained in this work from 'potential-jump' experiments. The relevant relationships are given by Eqn. 5a.

A quantitative analysis of the relaxation kinetics of the proton flow caused by a definite pNa-jump follows from the consideration of time derivatives of Eqn. 5. Since the buffering capacities for the sodium ions are much larger than those for the protons, the J_{H^+}-relaxation is measured at practically constant ΔpNa. In this case, we can write to a good approximation,

$$\frac{dJ_{H^+}}{dt} = -L_H\left(\frac{dpH^{ext}}{dt} - \frac{dpH^{int}}{dt}\right) \tag{10}$$

which leads to the same equation as that obtained for the relaxation of J_{H^+} after a ΔpH-jump. Thus we have Eqn. 9, for constant $\Delta\psi$, and when ΔpNa remains constant after the pNa-jump,

$$\frac{d\ln|J_{H^+}|}{dt} = +L_H\left(\frac{dpH^{int}}{dn_{H^+}^{int}} + \frac{dpH^{ext}}{dn_{H^+}^{ext}}\right) \tag{8}$$

According to the above, it is to be expected that the proton flows caused respectively by a pH-jump and by a pNa-jump will have the same relaxation constant (for the same L_H and conditions of identical pH-buffering capacities in the two types of experiments). The intercepts of the plots of $\ln J_{H^+}$ versus time evidently depend on the magnitudes of the pNa and pH jumps.

L_{Na} measurement

The parameter L_{Na} in Eqn. 4 is a straight overall thermodynamic permeability coefficient for Na^+-flow through the vesicle membrane. The value of L_{Na} in this system cannot be conveniently determined by the 'potential-jump' method (see Discussion). In this case, however, it could be conveniently determined from J_{Na^+} values and the known ΔpNa imposed across the membrane of the sub-bacterial particles. L_{Na} is then obtained as a differential parameter, by plotting the absolute values of J_{Na^+} versus the absolute values of ΔpNa. We have

$$L_{Na} = -\left(\frac{\partial J_{Na^+}}{\partial \Delta pNa}\right)_{\Delta pH=0,\Delta\psi=0} \tag{11}$$

As indicated by Eqn. 11 the experimental conditions correspond to $\Delta pH = 0$ and $\Delta\psi = 0$.

Materials and Methods

Cells of *Halobacterium halobium* were grown under aerobic conditions in the dark, in order to prevent the synthesis of the bacteriorhodopsin pigment. The growth conditions have already been described before [10]. The sub-bacterial particles were prepared from the above bacterial cultures, according to Ref. [10]. In all the preparations used, the salt concentrations both in the internal volume of the vesicles and in the external medium were 1 M NaCl and 2 M KCl. The preparations were kept at constant pH (between 6.5 and 7.0, for different preparations), using 0.5 mM Mes, Pipes and Hepes buffers in the external medium. In all the experiments the protein concentration was in the range of 7–14 mg/ml. The experiments were performed in thermostated tubes at 25°C, in the dark, and in the presence of DCCD (10^{-4} M) and azide (10^{-3} M). The first reagent was added in order to prevent proton leak through the ATPase system; the second was added in order to prevent possible back-flow of protons through the cytochrome system. $TPMP^+$ (10^{-3} M) was added to all the reaction mixtures, in order to prevent the formation of electric-potential differences across the particle membrane. In the experiments in which Na^+-flow was measured, FCCP (10^{-5} M) was also added. The latter prevented the formation of pH-gradients that would have been formed due to coupling between the Na^+ and proton flows *.

The proton flow was determined by measuring the corresponding rates of pH changes in the external solution. These pH changes were experimentally calibrated to give changes in the amount of protons in the medium. The proportionality factor is the buffering capacity of the system (dn_{H^+}/dpH). A Radiometer (Copenhagen) pH-meter (type 64) and a Radiometer (type GK2321C) glass electrode were used. The pH-meter was also connected to a high-speed recorder (Varian A-25)

* The above drugs have been used here in accordance with accepted practice in our laboratory and elsewhere (see, for example, Ref. 21). The effectiveness of $TPMP^+$ for the purpose in hand is discussed below.

with a response time of 0.5 s.

The flow of sodium ions was determined with the aid of the $^{22}Na^+$ isotope. For this purpose sub-bacterial particles were incubated for 4–7 days with the isotope, at 4°C, until equilibrium was obtained. Gradients in the chemical potential of the sodium ions were achieved by adding 3 M KCl solutions into the external medium. This procedure avoids the creation of gradients of the specific activity of $^{22}Na^+$. Under these experimental conditions, therefore, any change found in the vesicular radioactive counts represented net Na^+ flow. Special attention was paid to ensure that the added KCl solution was of the same pH and temperature as the vesicle suspension. Throughout the experiment, the suspension was vigorously stirred with a magnetic stirrer. Samples (20 μl) were taken at recorded intervals, transferred into a filtration device containing 10 ml of 3 M NaCl solution at 4°C, and were washed four times during a total of 30 s, using 3 ml aliquots of the cold suspension medium for each washing. Cellulose nitrate Millipore filters of 0.45 μm pore-size were used. The filter carrying the washed vesicles was transferred into a vial, and counted in a Packard γ-counter (model No. 578). Other samples (5–10 μl) were transferred without filtration to identical vials, to determine the specific activity of $^{22}Na^+$ of the medium.

The protein content was determined by the method of Lowry et al. [57], using bovine serum albumin as a standard.

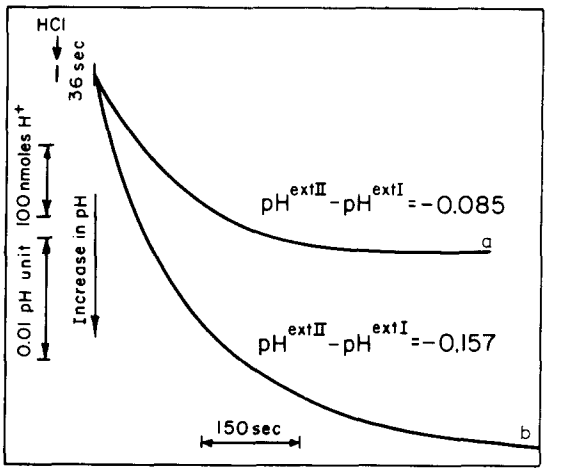

Fig. 1. Relaxation kinetics following a pH-jump. The sub-bacterial particles devoid of the purple membrane, were prepared by sonication in 1 M NaCl, 2 M KCl, 100 mM Mes, 100 mM Pipes and 100 mM Hepes. The vesicles were incubated in a solution of the same composition, but the concentration of each of the buffers was 0.5 mM. A sample of this suspension (9.9 mg protein/ml) was incubated in a thermostated vessel (25°C) together with DCCD (10^{-4}M), azide (10^{-3}M) and $TPMP^+$ (10^{-3}M), until equilibrium was reached. The pH-jump was produced by adding HCl (0.1 M) into the external medium. Two consecutive pH-jumps were performed. Curve a: Initial pH is 6.697 and the magnitude of the pH-jump is −0.085 pH units. Curve b: Initial pH is 6.913 and the magnitude of the pH-jump is −0.157 pH units. Note: Both curves are linear in the initial 36 s period.

Results

Determination of L_H

The experimental procedure for the determination of the value of L_H included (i) production of pH-jumps in the range of 0.05–0.3 units, and (ii) measurement of the proton-flow relaxation-kinetics. The changes in pH measured in the external solution were calibrated to give values of the corresponding changes in the proton content of the external solution. Sufficiently good stirring and use of a fast electrode are imperative to obtain satisfactory measurements that avoid overshoot artifacts. In some of our experiments a slight overshoot was indeed observed. It amounted to less than 5% of the total pH change, and relaxed within 1–2 s to a constant pH value which remained unchanged until recording ceased at least one minute later.

A typical pattern of proton relaxation kinetics induced by a given pH-jump is presented in Fig. 1. Values measured just immediately after the pH jump, during the first half-minute or so, fall on a practically straight line. Beyond this region the decay characteristics of the trace make themselves evident, as shown in the figure. The curves represent the later stages of relaxation toward higher values of pH^{ext} following the acidification at $t = 0$. A logarithmic plot of such data, in terms of Eqn. 7, is given in Fig. 2. The time in which KOH was added to the system is taken as $t = 0$. In this plot, the value of n^∞ was chosen so as to provide a best fit of the experimental results with linear logarithmic decay. As shown in Fig. 2, the experimental

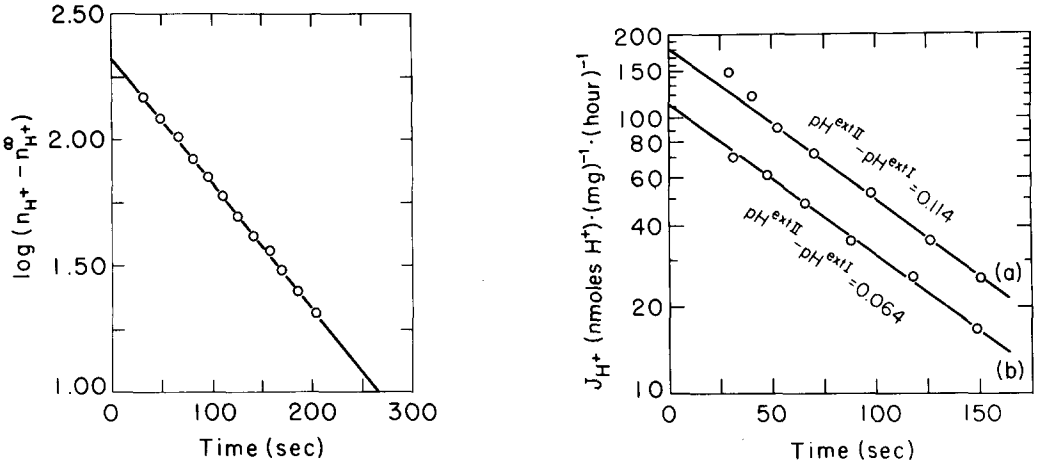

Fig. 2. Logarithmic analysis of the relaxation kinetics of the proton flow following a pH-jump. The preparation of the sub-bacterial particles is described in the legend to Fig. 1. Values of $(n_{H^+}^{ext} - n_{H^+}^{ext\infty})$ are plotted on a logarithmic scale vs. time, t, to check the validity of the Eqn. 7. (Arbitrary units are used for the n_{H^+} values, not affecting the value of the slope.)

Fig. 3. Logarithmic analysis of the relaxation kinetics of the proton flow following a pH-jump. The preparation of the sub-bacterial particles is described in the legend to Fig. 1. The proton flow, on a logarithmic scale, is plotted vs. time, t, to check the validity of Eqn. 8. Curve a: The proton flow following a pH-jump of 0.114 pH units (alkalinization with 0.1 M KOH). Curve b: The proton flow following a pH-jump of −0.064 pH units (acidification with 0.1 M HCl).

results are consistent with a single relaxation process.

A slightly different analysis of the proton flow leads to Eqn. 8 which does not include the value of n^{∞}. Fig. 3 represents J_{H^+} decay data in terms of Eqn. 8. The values of J_{H^+} were determined from the derivatives of the dependence of the external pH on time. The changes of pH were calibrated to provide values for the corresponding changes in the proton content of the external solution. The proportionality factor between the changes in proton content and changes in pH is the buffering capacity, which was measured under the conditions prevailing in each experiment. Results are presented for both positive and negative flows brought about by the addition of acid and base, respectively, to the external solution. As seen in Figs. 2 and 3, the observed relaxation kinetics can be satisfactorily described as single logarithmic decays of J_{H^+}. The two plots in Fig. 3 are seen to be parallel, indicating complete symmetry of the membrane with regard to the behavior of the ΔpH-driven proton-flow in the two directions. Extrapolation to $t = 0$ provides the required values of J_{H^+} and pH for the calculation of L_H. The dependence of $|\Delta J_{H^+}^{(II-I)}|$ on $|(pH^{ext\ II} - pH^{ext\ I})|$, at $t = 0$, is presented in Fig. 4. The value of L_H is given by

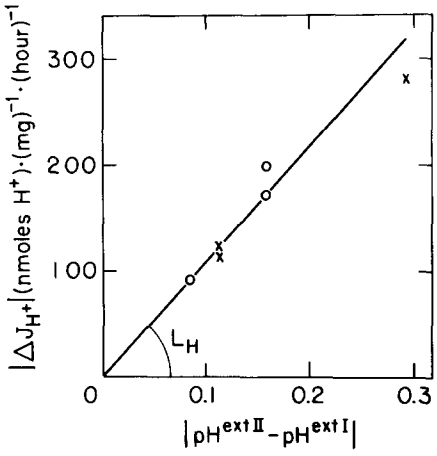

Fig. 4. Dependence of the change of the initial rate of proton flow on the magnitude of the pH-jump. This figure is a summary of several experiments of the type presented in Fig. 3, using the same sub-bacterial particle preparation. The pH-jumps were obtained by adding either KOH (0.01 M) or HCl (0.1 M), in an alternating sequence, into the vesicle suspension. The average pH was 6.8. (X) A positive pH-jump (alkalinization); (O) A negative pH-jump (acidification).

the slope of the latter plot. For the specific sub-bacterial particle preparation presented in this figure we find that $L_H = 1157 \pm 95.5$ (S.D.) nmol · (mg protein)$^{-1}$ · h^{-1} · (pH unit)$^{-1}$. Similar studies of different sub-bacterial preparations have shown that the respective average L_H values fall in the range of 850–1160 nmol H^+ · (mg protein)$^{-1}$ · h^{-1} · (pH unit)$^{-1}$ for four different preparations.

Determination of L_{HNa}

According to Eqn. 3, L_{HNa} is a parameter that characterizes the effect of ΔpNa on the proton flow (see also Eqn. 9); its non-zero value indicates that the proton and Na^+ flows are coupled. As in the case of L_H, L_{HNa} was evaluated from 'potential-jump' measurements (see Eqn. 5). The pNa-jumps were performed as follows: 3 M NaCl solution was added to the vesicle suspension that had been previously at equilibrium with 1 M NaCl + 2 M KCl *. Both solutions were at the same pH and temperature. The flows of the ions in the system are described schematically in Fig. 5.

Typical kinetics of proton flow induced by a pNa-jump are presented in Fig. 6. As in the case shown in Fig. 1, values measured immediately after the jump fall on a practically straight line. Logarithmic plots of J_{H^+} vs. time are shown in Figs. 7 and 8. The linear plots obtained are consistent with a single relaxation process. Fig. 7 presents the relaxation kinetics of J_{H^+}, observed in three different experiments with three different, fixed, values of ($pNa^{ext\ II} - pNa^{ext\ I}$). As expected

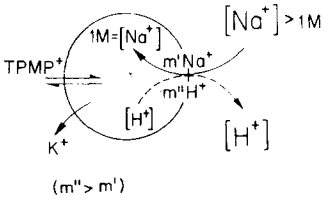

Fig. 5. A schematic presentation of the flow of electric charge and of ions in an experimental study of ΔpNa-driven proton-transport. m' and m'' are the 'stoichiometric-coefficients' of the H^+-Na^+ exchange, respectively. We have $m'' > m'$.

* Because of changes in the activity coefficients of NaCl and KCl, the concentration of total chloride has to be adjusted in order to maintain iso-osmotic conditions. In our experiments, the pNa-jumps involved iso-osmotic conditions, within the range of experimental error.

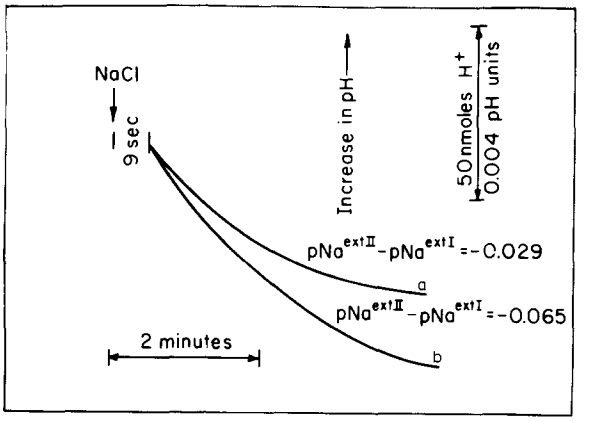

Fig. 6. ΔpNa-driven proton transport. The sub-bacterial particles (9.87 mg/ml, pH 6.5) were prepared as described in the legend to Fig. 1. The experiment was initiated by adding a 3 M NaCl solution into the incubation vessel, leading to $pNa^{ext\ II} - pNa^{ext\ I} = -0.065$. The resulting relaxation of the pH in the medium is shown in the curve b. The next pNa-jump was made immediately after the above, by adding more of the 3 M NaCl solution, so that $pNa^{ext\ II} - pNa^{ext\ I} = -0.029$. The resulting relaxation of pH in the medium is shown in curve a. The added NaCl solutions contained 0.5 mM Mes, 0.5 mM Pipes, and 0.5 mM Hepes. The added solutions were at the same temperature and pH as the vesicle solution. The initial pH before the pNa-jump represented in curve b was 6.608. The addition of NaCl solution caused an immediate pH-jump of +0.006 units. The initial pH before the pNa-jump represented in curve a was 6.600. The addition of the NaCl solution caused an immediate pH-jump of +0.011 units. Note: Both curves are linear in the initial 9 s period.

from Eqn. 8 the three lines have the same slope (i.e. the same proton buffering capacity), but have different intercepts, since the latter depend on the magnitude of the pNa and pH jumps. Eqn. 8 describes proton-flow relaxation kinetics observed in experiments involving a pH-jump and/or a pNa-jump. Fig. 8 presents the logarithmic decay of J_{H^+} following a pNa-jump (curve a), and a similar decay following a subsequent pH-jump (curve b). The two straight lines are seen to fit very closely the requirement that they should be parallel. It may be noted that the slopes in Figs. 7 and 8 are not identical. If Eqns. 7 and 8 are applicable, this is due to differences in buffering capacities for protons and/or in L_H-values in the respective experiments, as a consequence of differences in the preparations used. The graphs in the respective figures were chosen to indicate the ranges of val-

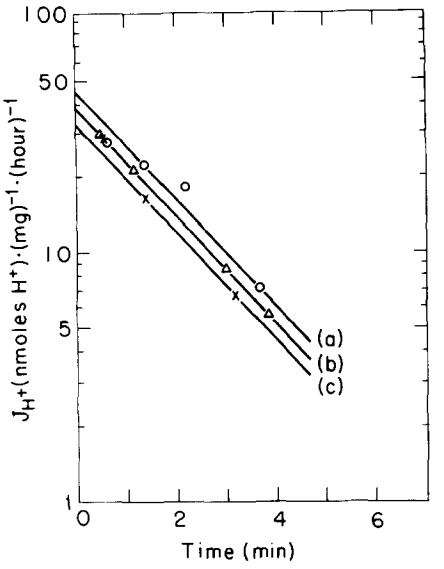

Fig. 7. Logarithmic analysis of the kinetics of the proton flow following a pNa-jump. The preparation of the sub-bacterial particles is described in the legend to Fig. 1. The proton flow (on a logarithmic scale) is plotted vs. time, to check the validity of Eqn. 8. Curve a: the pNa-jump is 0.065 units (negative). The initial pH before the pNa-jump is 6.608. The addition of the 3 M NaCl solution caused an immediate pH-jump of 0.006 pH units (alkalinization). Curve b: The pNa-jump is 0.029 units (negative). The initial pH before the pNa-jump is 6.600. The addition of the 3 M NaCl solution caused an immediate pH-jump of 0.011 pH units (alkalinization). Curve c: The pNa-jump is 0.018 units (negative). The initial pH before the pNa-jump is 6.612. The addition of the 3 M NaCl solution caused an immediate pH-jump of 0.018 units (alkalinization).

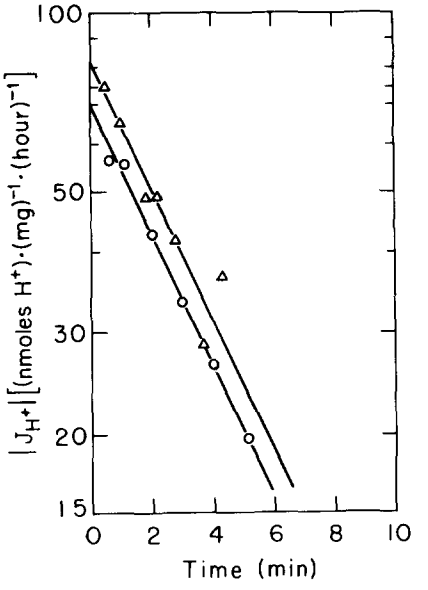

Fig. 8. Logarithmic analysis of the kinetics of the proton flow after a pNa-jump followed by a subsequent pH-jump. The preparation of the sub-bacterial particles is described in the legend to Fig. 1. The proton flow is plotted on a logarithmic scale vs. time, t, to check the validity of Eqn. 8. Curve a: The initial pH before the pNa-jump was 6.607. The magnitude of the pNa-jump was 0.0939 units (negative). The addition of the NaCl solution caused an immediate pH-jump of +0.009 pH units (alkalinization). Curve b: The initial pH before the pH-jump was 6.717. The pH-jump was −0.086 pH units (acidification).

ues encountered (see also Table I below). Extrapolation of J_{H^+} and pH to $t = 0$, obtained in the pNa-jump experiments (see Fig. 7), provided values of $\Delta J_{H^+}^{II\text{-}I}$ and ($pH^{ext\ II} - pH^{ext\ I}$) required for the calculations of L_{HNa}. A plot of the difference in the rates of proton flow $\Delta J_{H^+}^{II\text{-}I}$ (before and after the pNa-jump) versus the magnitude of the pNa-jump ($pNa^{ext\ II} - pNa^{ext\ I}$), is presented in Fig. 9. $\Delta J_{H^+}^{II\text{-}I}$ was corrected for the small variations in pH before and after the addition of the NaCl solution (approx. 0.01 pH units), according to Eqn. 5a, using the independently established values of L_H. The contribution of ΔpH to the measured $\Delta J_H^{I\text{-}II}$ was 20% upon the initial additions of NaCl solutions, and approached 70% upon further additions. The slope of the straight line in Fig. 9 is L_{HNa}. According to Fig. 9, $L_{HNa} = 588 \pm 183$ (S.D.) nmol $H^+ \cdot (mg\ protein)^{-1} \cdot h^{-1} \cdot (pNa\ unit)^{-1}$. The aver-

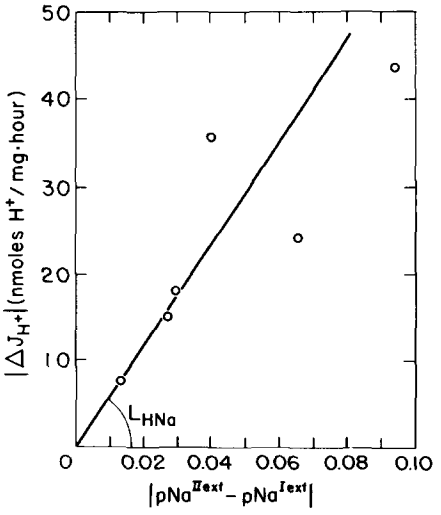

Fig. 9. Dependence of the initial proton flow on the magnitude of the pNa-jump. This figure summarizes several experiments of the type presented in Figs. 6 and 7. All the pNa-jumps were obtained by adding a 3 M NaCl solution into the external medium ($(pNa^{ext\ II} - pNa^{ext\ I}) < 0$).

age values of L_{HNa} obtained for four different sub-bacterial particle preparations were in the range of 220–590 nmol $H^+ \cdot (mg\ protein)^{-1} \cdot h^{-1} \cdot (pNa\ unit)^{-1}$.

Determination of L_{Na}

The parameter L_{Na}, the total straight thermodynamic overall permeability coefficient for Na^+-flow through the vesicle membrane, was determined according to Eqn. 11. For this purpose, the vesicle preparations used were initially at equilibrium with 1 M NaCl, 2 M KCl and $^{22}Na^+$. Gradients in the chemical potential of sodium ions were set up in one direction only, by adding a 3 M KCl solution to the external medium (see Methods). The amounts of vesicular sodium ions were determined using $^{22}Na^+$ as a tracer. In these experiments the specific activity of $^{22}Na^+$ is constant throughout the whole system. The values of L_{Na} have been determined from Na^+-efflux experiments only *. In these experiments bulk electroneutrality was maintained by Na^+-K^+ exchange since these are the predominant cations present. Such exchange may create a 'bi-ionic' electric potential gradient which is suppressed by the highly permeant $TPMP^+$ present in the system. At $\Delta\psi = 0$ we also have $\Delta pH = 0$, because of the presence of FCCP (10^{-5} M). The flows involved in these experiments are shown in Fig. 10. $TPMP^+$ is known to respond relatively slowly to changes in $\Delta\psi$, and in such circumstances control experiments are necessary to establish whether the stationary state has been reached. The reason for the slow response is the need for readjustment in $TPMP^+$ concentration on both sides of the membrane, which requires bulk flow. It should be pointed out that in our experiments this is not the case, since $TPMP^+$ is used for short-circuiting only, so that the stationary final conditions involve no changes in $TPMP^+$ concentration and no bulk flow of $TPMP^+$ occurs. Here the relaxation time for short-circuiting involves membrane polarization only and of course is very fast.

Representative results showing the net-efflux

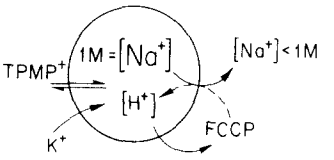

Fig. 10. A schematic presentation of ionic flows in an experiment of 'ΔpNa-driven J_{Na^+}'.

kinetics of sodium ions are given in Fig. 11. The typical pattern observed was that of a short initial retardation of the Na^+-efflux, followed by an exponential decay over a period exceeding 100 min. The retardation step was not always reproducible. The reason for the transient retardation step is not

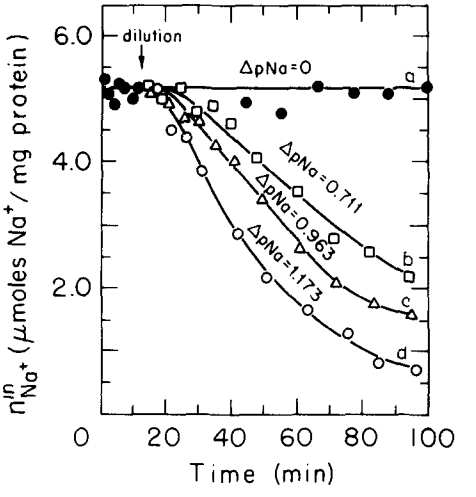

Fig. 11. Relaxation kinetics of the Na^+-flow following a pNa-jump. The sub-bacterial particles were prepared as described in the legend to Fig. 1, with the exception that the concentration of each of the buffers in the external solution was 50 mM. In addition, $^{22}Na^+$ was added into the external medium. After equilibration with the external solution for several days, the cells were introduced into a thermostated vessel (25°C), and azide (10^{-3}M), DCCD (10^{-4}M), $TPMP^+$ (10^{-3}M) and FCCP (10^{-5}M) were added. The pNa-jump was performed by transferring portions of the vesicle suspension into different volumes of 3 M KCl solutions which had been prepared earlier and kept inside thermostated vessels (25°C). The pH of the KCl solution was the same as that of the vesicle solution (pH = 6.5). Decrease of the amount of the $^{22}Na^+$ inside the vesicles was measured as a function of time. The separation between vesicles and medium was made by filtration. (□) 5.14-fold dilution of $n^{ext}_{Na^+}$ (ΔpNa = 0.711, curve b); (△) 9.27-fold dilution of $n^{ext}_{Na^+}$ (ΔpNa = 0.963, curve c); (○) 14.89-fold dilution of $n^{ext}_{Na^+}$ (ΔpNa = 1.173, curve d); (●) Control experiment (ΔpNa = 0, curve a).

* The values of L_{Na} obtained in these experiments are fully consistent with the values of Na^+-permeability obtained from measurements of $^{22}Na^+$-influx under zero gradient of bulk Na^+-concentration (see Ref. 9).

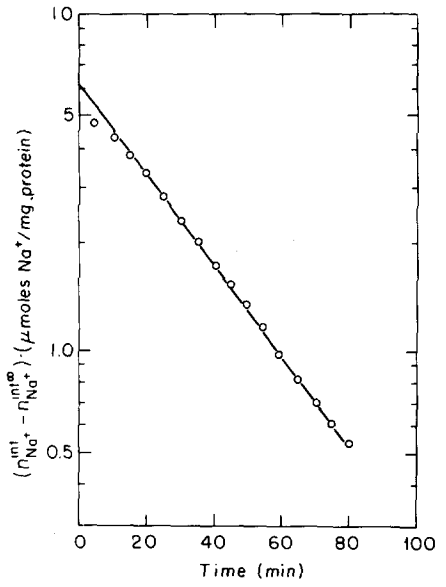

Fig. 12. Logarithmic analysis of the net Na^+-efflux kinetics. The plot is based on the data given in Fig. 11 ($\Delta pNa = 1.173$). The ordinate represents $(n_{Na^+} - n^{\infty}_{Na^+})$ on a logarithmic scale where n_{Na^+} is the total amount of Na^+ determined in the vesicles, and $n^{\infty}_{Na^+}$ is the equilibrium value at $t = \infty$, obtained by dividing the initial value of n_{Na^+} by the dilution factor (14.89).

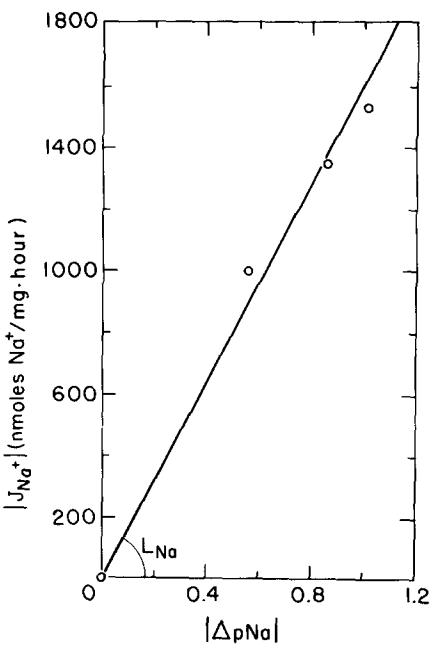

Fig. 13. Dependence of the initial rate Na^+-flow on the magnitude of the pNa-jump. This figure summarizes several experiments of the same type as that described in Fig. 11. The preparation of the sub-bacterial particles was the same as described in the legend to Fig. 11.

clear. Special checks were made to ensure that the pH and temperature of the added KCl solution were the same as those of the vesicle solutions, and that complete mixing had been obtained. Fig. 12 shows a logarithmic representation of the data given in Fig. 11. It is found that the ΔpNa-driven Na^+-flow after the initial retardation period can be described by single first-order relaxation kinetics. In complete analogy to Eqn. 7, we consider in this case the following expression (for $\Delta\psi = 0$, $\Delta pH = 0$):

$$\frac{d \ln(n_{Na} + n^{\infty}_{Na^+})}{dt} = L_{Na}\left(\frac{pNa^{ext} - pNa^{ext\infty}}{n^{ext}_{Na^+} - n^{ext\infty}_{Na^+}} + \frac{pNa^{int} - pNa^{int\infty}}{n^{int}_{Na^+} - n^{int\infty}_{Na^+}}\right) \equiv -K_{Na} \quad (12)$$

where n_{Na^+} and $n^{\infty}_{Na^+}$ are the vesicular amounts of sodium ions at time t, and at time $t = \infty$, respectively. According to the plot in Fig. 12, the product on the right-hand side of Eqn. 12 is constant.

The dependence of the initial value of Na^+-flow on initial $\Delta pNa^{ext\text{-}in}$ (taking the onset of the exponential decay as $t = 0$) is presented in Fig. 13. The slope of the plot in the above figure represents L_{Na}. In this case we find that $L_{Na} = 1622 \pm 173$ (S.D.) nmol $Na^+ \cdot (mg\ protein)^{-1} \cdot h^{-1} \cdot (pNa\ unit)^{-1}$. The average values of L_{Na} obtained for four different preparations of the sub-bacterial particles were in the range of 1620–2500 nmol $Na^+ \cdot (mg\ protein)^{-1} \cdot h^{-1} \cdot (pNa\ unit)^{-1}$.

Discussion

The potential-jump method provided a convenient experimental approach for the determination of the flow characteristics of protons and sodium ions in the sub-bacterial particles of *H. halobium*. This method made it possible to make no recourse to measurement of the chemical potentials within the vesicles. Measurement of changes in the flow, following the imposed jumps in pH or in pNa in the external solution, has two additional advantages. The experiments may be performed on a

system that need not be at equilibrium, and the measurement of changes in flows, and not of the absolute values, may significantly reduce errors arising, for example, from drifts in the system.

It has been pointed out that known, constant buffering capacities may be of great advantage in interpreting the results for ΔpH relaxation [55,56]. In our case special attention to this point was unnecessary, since the decay was logarithmic under the prevailing conditions. This enabled us to extrapolate the data to $t = 0$ satisfactorily, so that the initial change in proton flow could be established and the corresponding change in ΔpH checked.

The characteristics of the proton and sodium ion flows can be summarized as follows:

(1) The relaxation kinetics of the proton flow, observed both in the pH-jump and in the pNa-jump experiments, follow a single exponential decay (Figs. 2,3,7,8). This single exponential relaxation observed in the two types of jumps arises because of the fact that in both cases ΔpNa remains practically constant throughout the experiment, so that only one driving force, ΔpH, affects the relaxation process. The value of ΔpNa remains constant since the flow of the sodium ions, unlike that of the protons, does not affect the pNa values significantly, because of the relatively much higher concentrations of sodium ions both inside the particles and in the external medium. Thus any change in ΔpNa produced in the pNa-jump experiment leads to a change in J_{H^+} from some original value $J^{I}_{H^+}$ to a new value $J^{II}_{H^+}$. However, $J^{II}_{H^+}$ does not remain constant because its very existence introduces changes in ΔpH which lead to a decay of J_{H^+}. Finally, 'static head' conditions [40,51,52] may be reached, when $J_{H^+} = 0$, $\Delta pH \neq 0$, while ΔpNa has remained constant due to the high pNa-buffering capacity.

(2) The same values have been obtained for the decay constant of J_{H^+} in different experiments using different magnitudes of pH and pNa jumps (Figs. 3,7,8). This is consistent with the fact that the physical meaning of the decay constant, K_H, for the J_{H^+}-relaxation is the same in the above pH-jump and pNa-jump experiments. In all cases $K_H = L_H[(dpH^{ext}/dn^{ext}_{H^+}) + (dpH^{in}/dn^{in}_{H^+})]$.

(3) The intercepts of the plots of ln J_{H^+} vs. time (Figs. 3,7,8) provide (extrapolated) values of J_{H^+} at $t = 0$, immediately after the pH-jump. The difference, ΔJ_{H^+}, between these values and those measured before the potential-jump at $t = 0$ is found to be proportional to the magnitude of the pH-jump and of the pNa-jump (Figs. 4,9). Thus, the linear representation (Eqns. 3 and 4) is fully justified. The corresponding proportionality factors are the straight and cross-permeabilities, L_H and L_{HNa}, respectively. Measurement of differences of J_{H^+}, ($pH^{ext\ II} - pH^{ext\ I}$), and ($pNa^{ext\ II} - pNa^{ext\ I}$), and the evaluation of L_H and L_{HNa} as differential parameters, eliminate errors that may be introduced when measuring absolute quantities.

(4) The parameter L_{NaH}, characterizing the effect of ΔpH (at $\Delta\psi = 0$) on the flow of sodium ions ($L_{NaH} = (\partial J_{Na^+}/\partial \Delta pH)_{\Delta\psi, \Delta pNa}$) has not been determined quantitatively. Measurements of L_{NaH} are much more difficult to perform than those of L_{HNa}. This is due to the much lower sensitivity of the tracer measurements of Na^+-flow, as compared to that of the pH-measurements used in the determination of the proton-flow. An additional difficulty in the determination of L_{NaH} arises because of the very low buffering-capacity for protons in the vesicle interior. The latter leads to a relatively fast disappearance of the pH-gradient as a driving force for the Na^+-flow. As a result, only small amounts of sodium ions are transported relative to the total Na^+-concentrations. In our subsequent considerations we shall therefore resort to Onsager's reciprocal relations, and assume $L_{NaH} = L_{HNa}$.

(5) The flow characteristics of practically all the sodium ions transported through the membranes under stationary conditions, following a pNa-jump, can be represented by a single exponential (Fig. 12). Any initial deviations from this behaviour involved negligible amounts of sodium ions, and relate (by definition) to transient conditions. The nature of the lag phase is not clear. The lag was not reproducible and did not appear at all in some of the experiments. Significantly, the J_{Na^+} values obtained by extrapolation of the exponential decay led to L_{Na} values consistent with those obtained from $^{22}Na^+$-influx measurements (at bulk $\Delta pNa = 0$) (see footnote in Determination of L_{Na}, p. 20).

(6) The extrapolated value of Na^+-flow at $t = 0$ caused by a pNa-jump was found to be propor-

tional to the corresponding initial ΔpNa across the vesicle membrane. The proportionality factor, L_{Na}, is thus seen to be constant in the ΔpNa range involved (Fig. 13). On a priori grounds one would not expect L_{Na} and the buffer capacity to remain constant over large changes in concentration. However, the points in Fig. 13 correspond to constant (high) Na^+-concentration inside the vesicles and varying (lower) Na^+ concentrations in the external medium. Under these conditions the mean Na^+ concentration remains practically constant. (The relevant mean concentration, $\bar{C}_{Na}$, is the logarithmic mean: $\bar{C}_{Na} = \Delta C_{Na}/\Delta \ln C_{Na}$ [52].) It should be noticed that in contrast to the above conditions, the points in Fig. 12 correspond to decreasing internal Na^+ concentration while the external (low) concentration is kept constant. In this case $\bar{C}_{Na}$ is far from being constant and decreases in the course of relaxation. This corresponds to a decrease in the value of L_{Na}. It can be readily ascertained that with decreasing internal Na^+ concentration the inverse buffering capacity increases, so that the product provides a constant K-value consistent with Fig. 12.

(7) Proton-flow relaxation-kinetics, observed in a pH-jump experiment (at ΔpNa = 0, $\Delta\psi = 0$), provide all the necessary information for the determination of the buffering capacity of protons within small particles [9].

Buffering capacities are discussed in the present paper mainly in the context of understanding the physical meaning of the relaxation constant K and its relation to the corresponding L-value. No attempt has been made to specifically study the internal buffering capacity by different experimental methods. This issue is clearly important in its own right and would merit a special study. However, it is of interest to illustrate the method of calculating buffer capacity on the basis of Eqn. 8. The method requires the following three steps:

(i) Determination of the buffering capacity of the external solution ($-(\mathrm{dpH^{ext}}/\mathrm{d}n^{ext}_{H^+})^{-1}$).

(ii) Determination of L_H. (The initial change in J_{H^+} is divided by the magnitude of the pH-jump.)

(iii) Determination of the slope, $-K_H$, of the linear plot of $\ln J_{H^+}$ vs. time.

The above values can now be introduced into Eqn. 8, so that the inverse of the internal buffering capacity is given by:

$$\frac{\mathrm{dpH^{int}}}{\mathrm{d}n^{int}_{H^+}} = -\frac{K_H}{L_H} - \frac{\mathrm{dpH^{ext}}}{\mathrm{d}n^{ext}_{H^+}} \qquad (8a)$$

As an example, we consider the J_{H^+}-relaxation shown in Fig. 3. This figure provides all the information necessary for the calculation of the internal H^+-buffering capacity of the vesicles *. The pH-jumps in this case are 0.114 and -0.064 pH units. The corresponding initial ΔJ_{H^+} values are -181.5 and 113.1 nmol $H^+ \cdot (\mathrm{mg\ protein})^{-1} \cdot h^{-1}$. For L_H, we find, in this case, $L_H = [\Delta J_H/(\mathrm{pH^{ext\,II}} - \mathrm{pH^{ext\,I}})] = 1673$ nmol $H^+ \cdot h^{-1} \cdot (\mathrm{pH\ unit})^{-1} \cdot (\mathrm{mg\ protein})^{-1}$. The slope of the graphs in Fig. 3 is $|K_H| = 45.74\ h^{-1}$. The reciprocal of the external buffering capacity, $|\mathrm{dpH^{ext}}/\mathrm{d}n^{ext}_{H^+}|$, was found to be equal to 0.00596 pH units $\cdot$ (mg protein) $\cdot$ (nmol $H^+)^{-1}$ (from a calibration of pH-changes caused by the addition of known amounts of acid or base). Introducing the above information into Eqn. 8a, $|\mathrm{dpH^{int}}/\mathrm{d}n^{int}_{H^+}|$ is calculated to be equal to 0.02138 pH units $\cdot$ (mg protein) $\cdot$ (nmol $H^+)^{-1}$, or 0.0577 pH units $\cdot$ (μl internal volume) $\cdot$ (nmol $H^+)^{-1}$. The inverse of the latter value gives an internal buffering capacity of 17.33 (nmol H^+) $\cdot$ (pH unit)$^{-1} \cdot$ (μl internal volume)$^{-1}$ (assuming 2.7 μl internal volume per mg protein [10]). The value obtained is indeed in the expected range. This may be compared with the buffering capacity of distilled water at pH 7.0, which is of the order of 10^{-3} nmol $H^+ \cdot (\mathrm{pH\ unit})^{-1} \cdot (\mu l)^{-1}$, and with the buffering capacity of the external solution which is 3.497 nmol $H^+ \cdot (\mathrm{pH\ unit})^{-1} (\mu l)^{-1}$. The higher value for the internal buffering capacity is evidently due to the higher buffer content in the interior of the vesicles as compared with the medium. The internal buffering capacity is obviously lower than that of the original preparation medium, since a great part of the buffer would be absorbed by the removed sub-cellular debris. It should be noted that the buffer was incorporated in the internal volume at the stage of the prepara-

* The buffering capacity of the external medium should also be available. Calibration of the latter quantity has also been required for the evaluation of J_{H^+} from changes in $\mathrm{pH^{ext}}$ with time.

tion of vesicles by sonication. The vesicles were subsequently kept in a solution whose buffer concentration was lower by a factor of 200 for up to 2 weeks. Tests of vesicle integrity performed after 2 weeks of storage showed that 90% of the vesicles remained intact [10]. While in these intact vesicles there may be some leakage of buffer from the internal volume, it appears that the main loss of buffer took place during preparation due to absorption to charged components being removed from the cell-suspension.

(8) The observed non-zero value for L_{HNa} provides quantitative information on the existing coupling between the proton and sodium-ion flows. However, the efficiency of energy conversion and related properties depend on ratios involving both straight and cross coefficients. Table I summarizes the ranges of values of the phenomenological coefficients, L_{ij}, determined for different preparations of the sub-bacterial particle membrane of *H. halobium*. These are subsequently used for the calculation of other parameters characterizing different aspects of coupling and energy conversion in the Na^+-H^+ exchange system.

(9) The determination of L-values in this system involved considerable experimental difficulties, such as the measurement of very small pH changes and very small radioactive signal changes. The results, therefore, primarily indicate the ranges to be expected under the given experimental conditions.

In principle the L-values may change with time, or when ionophores are added, or when gradient profiles are changed. In our experiments the same batch of sub-bacterial particles was used for the determination of L_H, L_{HNa}, and L_{Na}. The treatment was completely identical in all cases up to the stage of the final incubation. At this stage FCCP and more buffer were added to the vesicle suspension in the case of L_{Na} measurements. The reason for these additions was, clearly, to prevent ΔpH formation and to stabilize a constant pH in the external medium. The assumption made in combining the L-values into composite parameters is that the former retain their values under these different conditions.

A convenient parameter to describe the coupling phenomenon is the coupling coefficient, q, defined by [40,51,52]:

$$q^2 = \left(\frac{\partial J_{H^+}}{\partial J_{Na^+}}\right)_{\Delta\tilde{\mu}_{H^+}} \cdot \left(\frac{\partial J_{Na^+}}{\partial J_{H^+}}\right)_{\Delta\tilde{\mu}_{Na^+}} = \frac{L_{HNa}^2}{L_{Na} \cdot L_H} \qquad (13)$$

Its range varies from $q = 0$ for zero coupling, to $q = 1$ for full coupling. Supposing the L_{ij} values reported above form a set characterizing a real stationary state, we find that $q = 0.4$ or less for different vesicle preparations (see Table I for the range of L-values).

The coupling coefficient uniquely determines the maximal efficiency of energy conversion in the process of Na^+-extrusion by the proton flow. Maximal efficiency, η_{max}, is given, according to Kedem and Caplan [51], by:

$$\eta_{max} = q^2/\left(1+\sqrt{1-q^2}\right)^2 \qquad (14)$$

It is of interest to have at least an order-of-magnitude estimate of this quantity (and also of the efficacy parameters discussed below). If the coupling in the region of maximum efficiency is characterized by q values as calculated above, η_{max} is 5% or less, for different preparations of the vesicles. This rather low maximal efficiency indicates that the bacteria may have to maintain relatively high rates of proton efflux (caused by either respiration or by the light reaction), so that the proton influx via the dark passive pathways can maintain a given stationary Na^+-gradient (see, however, the reference below, to light-driven Na^+ flow). Thus, in the absence of any other mechanism of Na^+-extrusion against its electrochemical potential difference, a sodium chemical-potential difference of one pNa unit (at 'static head', i.e. $J_{Na} = 0$) can be maintained only if the bacteria are able to produce

TABLE I

RANGES OF VALUES OF THE PHENOMENOLOGICAL COEFFICIENTS, L_{ij}, DETERMINED FOR FOUR DIFFERENT PREPARATIONS OF THE SUB-BACTERIAL PARTICLE MEMBRANE OF *H. HALOBIUM*

No correlations could be established between the variations in the values of L_H, L_{HNa}, and L_{Na} in the different preparations.

L_H	= 1160– 850	nmol $H^+ \cdot mg^{-1} \cdot h^{-1} \cdot (pH\ unit)^{-1}$
L_{HNa}	= 590– 220	nmol $H^+ \cdot mg^{-1} \cdot h^{-1} \cdot (pNa\ unit)^{-1}$
L_{Na}	= 1620–2500	nmol $Na^+ \cdot mg^{-1} \cdot h^{-1} \cdot (pNa\ unit)^{-1}$

a pH-difference of almost three pH units, which corresponds to an influx of protons of about 3500 nmol $H^+ \cdot (mg\ protein)^{-1} \cdot h^{-1}$. These estimates are based on Eqns. 3 and 4. Such flows and pH-differences are in the range of experimentally found values in studies of the same preparation of the sub-bacterial particles under illumination (Cooper, S., unpublished results). It should be noticed that pathways involving Na^+-Ca^{2+} antiport and Na^+-amino-acid symport have not been blocked in our preparations, and may have served as leaks for J_{Na^+}, thus contributing to a lower efficiency calculated for the H^+-Na^+ exchange system. A large fraction of the power-input regarded as wasted in these calculations may actually be utilized in the Ca^{2+} and amino-acid transport. Heinz and Geck [48,49] analyzed the Na^+-α-aminoisobutyrate symport system in Ehrlich cells. These investigators found a maximal efficiency of 8% for this transport system. However, corrections for Na^+-flows coupled to other flows increased the above calculated efficiency by an order of magnitude. The only pathways blocked in our system were those affected by the addition of DCCD and azide. The latter prevent proton transport through the ATPase system and through some of the cytochrome sites.

Recent observations [29–32] indicate that Na^+-ions might be extruded against their electrochemical potential difference in a process directly driven by light. In this case, the required values of ΔpH and J_{H^+}, under illumination, may be lower than those given in the above estimates, and the Na^+-H^+ antiport need not be the main mechanism involved in maintaining the Na^+ gradient.

The existence of coupling between the Na^+ and proton flows raises the question of a possible 'mechanistic stoichiometry', r, in the coupling site. In the case of complete coupling (when $q = 1$), the mechanistic stoichiometry is given by the macroscopically measured flow-ratio ($r = J_{H^+}/J_{Na^+}$) which is constant for all conditions of flows and forces. However, when $q < 1$, as was found above, the flow-ratio is not constant, and depends on the force-ratio [52]. At $q < 1$, therefore, the mechanistic stoichiometry at the coupling site cannot be calculated. However, a range for the mechanistic stoichiometry can be estimated within definite limiting values. A lower limit for the mechanistic stoichiometry at the coupling site is given by L_{NaH}/L_{Na}:

$$r \geqslant -\left(\frac{J_{H^+}}{J_{Na^+}}\right)_{\Delta\tilde{\mu}_{H^+}=0} = \left(\frac{\Delta\tilde{\mu}_{Na^+}}{\Delta\tilde{\mu}_{H^+}}\right)_{J_{Na^+}=0} = \frac{L_{NaH}}{L_{Na}} \qquad (15)$$

An upper limit for the mechanistic stoichiometry at the coupling site is given by L_H/L_{HNa}:

$$r \leqslant -\left(\frac{J_{H^+}}{J_{Na^+}}\right)_{\Delta\tilde{\mu}_{Na^+}=0} = \left(\frac{\Delta\tilde{\mu}_{Na^+}}{\Delta\tilde{\mu}_{H^+}}\right)_{J_{H^+}=0} = \frac{L_H}{L_{HNa}} \qquad (16)$$

Introducing the L_{ij}-values reported above into the expressions for r, we find: $0.36 \leqslant r \leqslant 2$. As can be seen, the limits for r obtained from the experiments in the dark are rather broad. These limits permit the existence of either electroneutral or electrogenic exchange in either direction. It should be mentioned, however, that additional studies of Na^+-flows under illumination showing an inhibitory effect of excess $TPMP^+$ and of excess TPB^-, narrow down the above range for r to $1 < r \leqslant 2$, i.e. $r = 2$ (see Refs. 9,14).

Additional parameters of biological interest characterizing the H^+-Na^+ exchange system are the force and flow efficacies [52]. The 'force-efficacy' (ϵ_{X_1}) is defined as the electrochemical gradient (X_1) obtained at static head (when $J_1 = 0$), per unit of power input. In our system the 'force-efficacy' of sodium ions is defined as the Na^+-electrochemical potential difference obtained per unit of power-input due to the proton flow, and is given by:

$$\epsilon_{\Delta\tilde{\mu}_{Na^+}} = \left|\left(\frac{\Delta\tilde{\mu}_{Na^+}}{J_{H^+} \cdot \Delta\tilde{\mu}_{H^+}}\right)_{J_{Na^+}=0}\right| \qquad (17)$$

Transformation to units of ΔpNa per unit power-input of the proton flow leads to

$$\epsilon_{\Delta pNa} \equiv \left|\frac{\Delta pNa}{2.3 \cdot J_{H^+} \cdot \Delta pH}\right| = \left|\left[\left(1 - \frac{1}{q^2}\right) 2.3 \cdot L_{Na} \cdot \Delta pNa\right]^{-1}\right| \qquad (18)$$

at $\Delta\psi = 0$ in units of $\Delta pNa \cdot mg \cdot h \cdot (RT\ \text{unit of energy})^{-1}$, for L_{Na} taken in units of mol $Na^+ \cdot mg^{-1} \cdot h^{-1} \cdot (pNa\ unit)^{-1}$. The right hand side of this equation is obtained by straight-forward transformation of Eqns. 3, 4 and 13. One has to pay attention to the fact that the 'force-efficacy' is

not a constant parameter of a given system, but decreases with increasing values of the gradients of sodium ions at static head. For $\Delta pNa = 1$ unit, we find for our system that $\epsilon_{\Delta pNa} = 5 \cdot 10^4$ ($\Delta pNa \cdot mg \cdot h \cdot (RT$ unit of energy$)^{-1}$, or less, for different preparations.

An interesting quantity to consider is $1/\epsilon_{\Delta pNa}$, which is the power-input required to maintain one unit of ΔpNa (under conditions of $J_{Na} = 0$ at $\Delta\psi = 0$). We find $1/\epsilon_{\Delta pNa} = 2 \cdot 10^{-5}$ (RT units of energy)$\cdot(\Delta pNa)^{-1} \cdot (mg\ protein)^{-1} \cdot h^{-1}$, or more, for different preparations.

The 'flow-efficacy' of sodium ions is defined as the magnitude of the Na^+-flow under 'level-flow' conditions (when $\Delta\tilde{\mu}_{Na^+} = 0$) per unit of power-input due to the proton flow. The flow-efficacy of sodium ions is given by:

$$\epsilon_{J_{Na^+}} \equiv \left| \left(\frac{J_{Na^+}}{J_{H^+} \cdot \Delta\tilde{\mu}_{H^+}} \right)_{\Delta\tilde{\mu}_{Na^+}=0} \right| \tag{19}$$

or in units of mol per unit of RT,

$$\epsilon_{J_{Na^+}} \equiv \left| \frac{J_{Na^+}}{2.3 \cdot J_{H^+} \cdot \Delta pH} \right| = \left| \frac{L^2_{NaH}}{2.3 \cdot L_H \cdot J_{Na^+}} \right| \tag{20}$$

at $\Delta\psi = 0$, $\Delta pNa = 0$.

For $J_{Na^+} = 1\ \mu mol\ Na^+ \cdot mg^{-1} \cdot h^{-1}$, we find $\epsilon_{J_{Na^+}} = 0.13$ mol per RT unit of energy. Its inverse, $1/\epsilon_{J_{Na^+}}$, represents the power required to maintain one unit of J_{Na^+} (under conditions of $\Delta pNa = 0$ and $J_{Na^+} = 1\ \mu mol\ Na^+ \cdot (mg\ protein)^{-1} \cdot h^{-1}$). We find that the energy required to transport 1 mol Na^+ under the above conditions is 7.7 RT units of energy, or more, for different preparations.

References

1 Lanyi, J.K. and MacDonald, R.E. (1979) Methods Enzymol. 56, 398–407
2 Lanyi, J.K. (1979) Bacteriol. Rev. 38, 272–290
3 Brown, A.D. (1976) Bacteriol. Rev. 40, 803–846
4 Lanyi, J.K. (1980) Origins Life 10, 161–167
5 Eisenbach, M. and Caplan, S.R. (1979) in Current Topics in Membranes and Transport (Bronner, F. and Kleinzeller, A., eds.), Vol. 12, pp. 165–248, Elsevier/North-Holland, Amsterdam
6 Bayley, S.T. and Morton, R.A. (1978) CRC Crit. Rev. Microbiol. 6, 151–205
7 Lanyi, J.K. (1979) in Membrane Proteins in Energy Transduction (Capaldi, R.A., ed.), Vol. 2, pp. 451–483, Marcel Dekker, New York
8 Lanyi, J.K. (1978) Microbiol. Rev. 42, 682–706
9 Cooper, S. (1978) Ph.D. Thesis, Feinberg Grad. School, Weizmann Institute of Science, Rehovot, Israel
10 Eisenbach, M., Cooper, S., Garty, H., Johnstone, R.M., Rottenberg, H. and Caplan, S.R. (1977) Biochim. Biophys. Acta 465, 599–613
11 Caplan, S.R., Eisenbach, M., Cooper, S., Garty, H., Klemperer, G. and Bakker, E.P. (1977) in Bioenergetics of Membranes (Packer, L., Papageorgiou, G.C. and Trebst, A., eds.), pp. 101–114, Elsevier/North-Holland, Amsterdam
12 Cooper, S., Michaeli, I. and Caplan, S.R. (1978) in Energetics and Structure of Halophilic Microorganisms (Caplan, S.R. and Ginzburg, M., eds.), pp. 201–208, Elsevier/North-Holland, Amsterdam
13 Lanyi, J.K. and MacDonald, R.E. (1976) Biochemistry 15, 4608–4614
14 Lanyi, J.K., Renthal, R. and MacDonald, R.E. (1976) Biochemistry 15, 1603–1610
15 Lanyi, J.K. and MacDonald, R.E. (1977) Fed. Proc. 36, 1824–1827
16 Lanyi, J.K. (1977) J. Supramol. Struct. 6, 169–177
17 Lanyi, J.K. and Silverman, M.P. (1979) J. Biol. Chem. 254, 4750–4755
18 Renthal, R. and Lanyi, J.K. (1976) Biochemistry 15, 2136–2143
19 Eisenbach, M., Garty, H., Rottenberg, H. and Caplan, S.R. (1978) Biochemistry 17, 4691–4698
20 Lanyi, J.K., Helgerson, S.L. and Silverman, M.P. (1979) Arch. Biochem. Biophys. 193, 239–339
21 Bakker, E.P., Rottenberg, H. and Caplan, S.R. (1976) Biochim. Biophys. Acta 440, 557–572
22 Michel, H. and Oesterhelt, D. (1976) FEBS Lett. 65, 175–178
23 Wagner, G. and Hope, A.B. (1976) Aust. J. Plant Physiol. 3, 665–676
24 Bogomolni, R.A., Baker, R.A., Lozier, R.H. and Stoeckenius, W., (1976) Biochim. Biophys. Acta 440, 68–88
25 Bogomolni, R.A. (1977) Fed. Proc. 36, 1833–1839
26 Harold, E.M. and Altendorf, K. (1974) in Current Topics in Membranes and Transport (Bronner, F. and Kleinzeller, A., eds.),Vol. 5, pp. 1–49, Academic Press, New York
27 Harold, F.M. (1977) Annu. Rev. Microbiol. 31, 181–203
28 Lanyi, J.K. (1979) Biochim. Biophys. Acta 559, 377–397
29 Lindley, E.V. and MacDonald, R.E. (1979) Biochem. Biophys. Res. Commun. 88, 491–499
30 MacDonald, R.E., Lanyi, J.K., Greene, R.V. and Lindley, E.V. (1979) Biophys. J. 25, 205a
31 Lanyi, J.K. and Weber, H.J. (1980) J. Biol. Chem. 255, 243–250
32 Bogomolni, R.A. and Weber, H.J. (1980) Fed. Proc. 39, 1846
33 Schobert, B. and Lanyi, J.K. (1982) J. Biol. Chem. 257, 10306–10313
34 Lanyi, J.K., Yearwood-Drayton, V. and MacDonald, R.E. (1976) Biochemistry 15, 1595–1603
35 MacDonald, R.E. and Lanyi, J.K. (1977) Fed. Proc. 36, 1828–1832
36 Lanyi, J.K. (1978) Biochemistry 17, 3011–3018
37 Lanyi, J.K. (1978) Arch. Biochem. Biophys. 191, 821–824

38 Belliveau, J.W. and Lanyi, J.K. (1978) Arch. Biochem. Biophys. 186, 98–105
39 Westerhoff, H.V. and Van Dam, K. (1979) in Current Topics in Bioenergetics, (Sanadi, D.R., ed.), Vol. 9, pp. 1–62, Academic Press, New York
40 Stucki, J.W. (1980) Eur. J. Biochem. 109, 269–283
41 Pietrobon, D., Zoratti, M., Azzone, G.F., Stucki, J.W. and Walz, D. (1982) Eur. J. Biochem. 127, 483–494
42 Vieira, F.L., Caplan, S.R. and Essig, A. (1972) J. Gen. Physiol. 59, 77–91
43 Owen, A., Caplan, S.R. and Essig, A. (1975) Biochim. Biophys. Acta 394, 438–448
44 Essig, A. (1975) Biophys. J. 15, 651–665
45 Caplan, S.R. and Essig, A. (1977) in Current Topics in Membranes and Transport (Bronner, F. and Kleinzeller, A., eds.), Vol. 9, pp. 145–175, Academic Press, New York
46 Lahav, J., Essig, A. and Caplan, S.R. (1976) Biochim. Biophys. Acta 448, 389–392
47 Lahav, J. and Michaeli, I. (1978) J. Membrane Biol. 42, 1–18
48 Geck, P., Heinz, E. and Pfeiffer, B. (1972) Biochim. Biophys. Acta 288, 486–491
49 Heinz, E. and Geck, P. (1974) Biochim. Biophys. Acta 339, 426–431
50 Arents, J.C., Hellingwerf, K.J., Van Dam, K. and Westerhoff, H.V. (1981) J. Membrane Biol. 60, 95–104
51 Kedem, O. and Caplan, S.R. (1965) Trans. Faraday Soc. 61, 1897–1911
52 Caplan, S.R. (1971) in Current Topics in Bioenergetics (Sanadi, D.R., ed.), Vol. 4, pp. 1–79, Academic Press, New York
53 Mitchell, P. and Moyle, J. (1967) Biochem. J. 104, 558–600
54 Mitchell, P. (1969) in Theoretical and Experimental Biophysics (Cole, A., ed.), Vol. 2, pp. 159–216, Marcel Dekker, New York
55 Kell, D.B. and Morris, J.B. (1980) J. Biochem. Biophys. Methods, 3, 143–150
56 Arents, J.C., Van Dekken, H., Hellingwerf, K.J. and Westerhoff, H.V. (1981) Biochemistry 20, 5114–5123
57 Lowry, O.H., Rosebrough, N.J., Farr, A.L. and Randall, R.J. (1951) J. Biol. Chem. 193, 265–275